

Method of numerical simulation of interacting quantum gas kinetics on finite momentum lattice

I. O. Kuznetsov and P. F. Kartsev

*National Research Nuclear University MEPhI (Moscow Engineering Physics Institute),
115409, Russian Federation, Moscow, Kashirskoe hwy, 31*

We present the efficient and universal numerical method for simulation of interacting quantum gas kinetics on a finite momentum lattice, based on the Boltzmann equation for occupation numbers. Usually, the study of models with two-particle interaction generates the excessive amount of terms in the equations essentially limiting the possible system size. Here we employ the original analytical transformation to decrease the scaling index of the amount of calculations. As a result, lattice sizes as large as $48 \times 48 \times 48$ can be simulated, allowing to study realistic problems with complex interaction models. The method was applied to the simulation of weakly interacting Fermi and Bose gases where we calculated the relaxation times depending on the momentum and temperature.

PACS numbers: 71.10.Fd, 72.15.Lh, 67.85.Hj

I. INTRODUCTION

There are many problems concerning the time evolution of complex interacting quantum systems in modern physics. Examples in solid state physics include the behaviour of nonequilibrium charge carriers in semiconductors [1, 2] or metals [3, 4], the relaxation of an excited state in a superconductor [5, 6], the condensation of exciton polaritons [7, 8], and the dynamics of a Bose-Einstein condensate (BEC) in a reconfigurable quantum simulator [9].

To correctly describe such physical phenomena as formation of BEC state [10–13], relaxation of excited state of electron subsystem created by a ultrashort laser pulse [3, 14] or after absorbing cosmic particle [6], and many other promising applications, the detailed theoretical approaches are required. Popular analytical approaches include Boltzmann equation [15], nonequilibrium Green functions [16], Liouville equation [17], Fermi liquid theory [18], and others [14, 19, 20]. Application of purely analytical approaches to modern quantum problems, however, can be difficult due to complexity of the models and, therefore, numerical calculations are unavoidable [12].

The Boltzmann equation is efficient for numerical study of weakly interacting systems not far from equilibrium [4, 15, 21]. Here we present the efficient numerical method to study the kinetics of quantum systems of various statistics using the Boltzmann equation on a finite momentum lattice. The efficiency is achieved with the special analytical transformation, which is described in details. The method allows to take into account the energy exchange with thermal bath or nonequilibrium phonons as well as two-particle interaction, which usually requires high amount of calculations. The possibility to take into consideration arbitrary single-particle energies and level broadening factors enables to study extensive set of promising physical problems. The operation of the method is demonstrated by the calculation of relaxation times in weakly interacting Bose and Fermi gases.

II. FINITE MOMENTUM LATTICE

In this work, we present the numerical method to simulate the kinetics of a sufficiently small system, a finite atomic cluster or nanocrystal. For certainty, let consider a nanocrystal of $L \times L \times L$ atoms with a simple cubic lattice (generalizations for other lattices are obvious). The number of points in the reciprocal lattice is also $L \times L \times L$ with the step $\Delta k = 2\pi/La$, where a is the lattice constant.

The Hamiltonian of the system is taken in the form:

$$\hat{H} = \hat{H}_1 + \hat{H}_{\text{int}}, \quad (1)$$

$$\hat{H}_1 = \sum_{\mathbf{k}} \varepsilon_{\mathbf{k}} \hat{n}_{\mathbf{k}}, \quad (2)$$

where \hat{H}_1 and \hat{H}_{int} are the single-particle Hamiltonian and interaction part, correspondingly, $\varepsilon_{\mathbf{k}}$ are particle energies, $\hat{n}_{\mathbf{k}}$ is the operator of occupation number. Index \mathbf{k} also includes a spin index in the case of fermions. For complicated problems, additional sorts of particles can be introduced by relevant terms in the Hamiltonian (1), for example, phonons to account for the interaction with the lattice.

The kinetics of the system due to interaction is described by the Boltzmann equation [22] derived from Fermi's Golden rule:

$$\frac{1}{\tau_{\mathbf{k}}} = \frac{2\pi}{\hbar} \sum_{i,f} \langle i | \hat{H}_{\text{int}} | f \rangle^2 \delta(E_i - E_f), \quad (3)$$

where $\langle i | \hat{H}_{\text{int}} | f \rangle$ are the matrix elements of interaction operator between initial i and final f states changing the occupation $n_{\mathbf{k}}$. Later on, for simplicity, we use the time units where $2\pi/\hbar = 1$.

The application of Boltzmann equation to continual problems comes down to performing integrations with the particle density on the energy axis [4, 6]. In the case of a nanocluster with finite momentum step, however, the numerical summation of the original expressions should

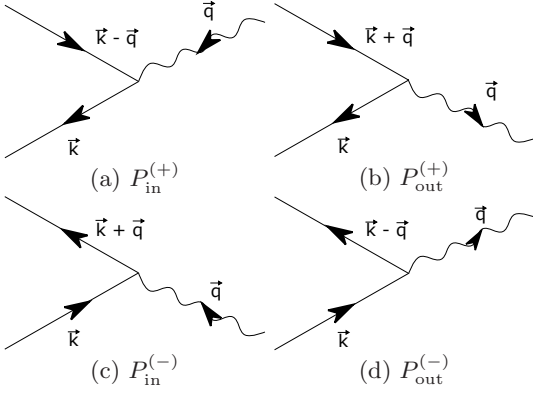


Figure 1: The processes for the corresponding terms in Eq. (5) generated by the interaction with phonons: adding or removing particle with momentum \mathbf{k} and phonon with momentum \mathbf{q} .

be used. On the other side, the number of terms rapidly grows with the lattice size L and sizes $L > 8$ are practically untractable [23].

In this section we present a convenient and efficient way to extend possible system sizes up to $L \sim 32 \div 48$ using a special transformation. This allows simulations of large enough sizes for subsequent extrapolation to the continual limit $L \rightarrow \infty$. As a result, new physical problems can be studied which could not be explored by the aforementioned analytical methods.

a. Interaction with the phonon subsystem. We begin with a simple case: a system of free particles in the presence of phonons (crystal lattice with given temperature T):

$$\hat{H}_{\text{int,phon}} = M_0 \sum_{\mathbf{k}\mathbf{q}} \hat{a}_{\mathbf{k}}^\dagger \hat{a}_{\mathbf{k}-\mathbf{q}} \hat{b}_{\mathbf{q}} + H.c., \quad (4)$$

where $\hat{a}_{\mathbf{k}}$, $\hat{a}_{\mathbf{k}}^\dagger$ and $\hat{b}_{\mathbf{q}}$, $\hat{b}_{\mathbf{q}}^\dagger$ are operators of particles under consideration and phonons, correspondingly, and M_0 is the matrix element of interaction with phonons. In the case of Fermi particles, spin index is for simplicity included in the particle momentum \mathbf{k} .

In Figure 1, we show the processes generated by this type of interaction that change the number of particles $n_{\mathbf{k}}$ and phonons $n_{\mathbf{q}}^{(\text{phon})}$. The corresponding terms in the kinetic equations according to (3) in the case of Bose statistics have the form:

$$\begin{aligned} \frac{dn_{\mathbf{k}}}{dt} &= P_{\text{in}}^{(+)} + P_{\text{out}}^{(+)} - P_{\text{in}}^{(-)} - P_{\text{out}}^{(-)}, \quad (5) \\ P_{\text{in}}^{(+)} &= M_0^2 \sum_{\mathbf{q}} (n_{\mathbf{k}} + 1) n_{\mathbf{k}-\mathbf{q}} n_{\mathbf{q}}^{(\text{phon})} F(\delta E), \\ P_{\text{out}}^{(+)} &= M_0^2 \sum_{\mathbf{q}} (n_{\mathbf{k}} + 1) n_{\mathbf{k}+\mathbf{q}} (n_{\mathbf{q}}^{(\text{phon})} + 1) F(\delta E), \\ P_{\text{in}}^{(-)} &= M_0^2 \sum_{\mathbf{q}} n_{\mathbf{k}} (n_{\mathbf{k}+\mathbf{q}} + 1) n_{\mathbf{q}}^{(\text{phon})} F(\delta E), \\ P_{\text{out}}^{(-)} &= M_0^2 \sum_{\mathbf{q}} n_{\mathbf{k}} (n_{\mathbf{k}-\mathbf{q}} + 1) (n_{\mathbf{q}}^{(\text{phon})} + 1) F(\delta E), \end{aligned}$$

where phonon energies are denoted $\tilde{\varepsilon}_{\mathbf{q}}$ and δE is the corresponding energy difference for incoming and outgoing particles. The factor $F(\delta E)$ is introduced to account for the finite width of the energy levels. The four given terms correspond to the various types of interaction with phonon absorption or radiation, as shown in Figure 1. In the case of Fermi statistics, $(n + 1)$ is replaced with $(1 - n)$.

Depending on the problem under study, the phonon subsystem can be taken into account in two ways: considering phonons as equilibrium (thermal bath) or nonequilibrium. For equilibrium phonons, their occupation numbers are determined by the Bose-Einstein distribution function $n_{\mathbf{q}}^{(\text{phon},0)} = f(\tilde{\varepsilon}_{\mathbf{q}}, T)$, here T is the temperature. In the case of nonequilibrium phonons, the system (5) is supplemented with similar equations for the phonon numbers, and finite phonon lifetime $\tau^{(\text{phon})}$ related to their decay in the area of consideration is taken into account:

$$P_{\text{dec}}^{(\text{phon})} = -\frac{1}{\tau^{(\text{phon})}} \left(n_{\mathbf{q}}^{(\text{phon})} - n_{\mathbf{q}}^{(\text{phon},0)} \right). \quad (6)$$

The interaction with the phonon subsystem is crucial when the pair interaction is negligible, for example, at low particle density.

b. Two-particle interaction. However, the interaction with phonons alone is often not enough to correctly describe kinetic phenomena in complex systems, and it is necessary to take into account the processes due to the interaction between particles [4].

We write the two-particle interaction as:

$$\hat{H}_{\text{int,pair}} = \sum_{\mathbf{k}\mathbf{p}\mathbf{q}} U(\mathbf{q}) \hat{a}_{\mathbf{k}}^\dagger \hat{a}_{\mathbf{p}}^\dagger \hat{a}_{\mathbf{p}+\mathbf{q}} \hat{a}_{\mathbf{k}-\mathbf{q}} \quad (7)$$

Next, for convenience, we denote the momenta of four particles involved in the interaction \mathbf{k} , \mathbf{p} , $\mathbf{p} + \mathbf{q}$, $\mathbf{k} - \mathbf{q}$ as $\mathbf{1}$, $\mathbf{2}$, $\mathbf{3}$, $\mathbf{4}$, correspondingly, and show the conservation law explicitly with Kronecker delta:

$$\hat{H}_{\text{int,pair}} = \sum_{\mathbf{1234}} U_{\mathbf{3-2}} \hat{a}_{\mathbf{1}}^\dagger \hat{a}_{\mathbf{2}}^\dagger \hat{a}_{\mathbf{3}} \hat{a}_{\mathbf{4}} \delta_{\mathbf{1}+\mathbf{2},\mathbf{3}+\mathbf{4}} \quad (8)$$

Then, kinetic equations take the form:

$$\frac{dn_1}{dt} = \sum_{\mathbf{234}} |U_{\mathbf{3-2}}|^2 [(n_1 + 1)(n_2 + 1 + \delta_{12})n_3(n_4 - \delta_{34}) - n_1(n_2 - \delta_{12})(n_3 + 1)(n_4 + 1 + \delta_{34})] \delta_{\Delta\varepsilon,0} \delta_{\mathbf{1+2,3+4}} \quad (9)$$

for Bose statistics and

$$\frac{dn_1}{dt} = \sum_{\mathbf{234}} |U_{\mathbf{3-2}}|^2 [(1 - n_1)(1 - n_2 - \delta_{12})n_3(n_4 - \delta_{34}) - n_1(n_2 - \delta_{12})(1 - n_3)(1 - n_4 - \delta_{34})] \delta_{\Delta\varepsilon,0} \delta_{\mathbf{1+2,3+4}} \quad (10)$$

for Fermi statistics, respectively.

We should note the corrections using δ_{12} , δ_{34} in the terms with coinciding momenta. While they are negligible in the continual case, for a finite system the exact form is essential.

As we mentioned earlier, the practical use of the expressions (9), (10) on the momentum lattice $L \times L \times L$ is hindered by the necessity to calculate a large number of terms which can be estimated as $\sim V^4 = L^{12}$, and as a result, the simulation of system with lattice size $L > 8$ is practically impossible [23, 24]. However, in the model of the form (7), when the total momentum is conserved, we can use the analytical transformation working in the extended space $(\mathbf{k}, \varepsilon)$ of size $L^3 \times N_\varepsilon \sim L^5$ that dramatically reduces the amount of calculations to $\sim L^5 \ln L$. It allows to greatly increase the affordable system sizes.

c. Free gas case. We demonstrate the principle of this transformation using the example of a free gas of Fermi or Bose particles with the energy spectrum $\varepsilon_{\mathbf{k}} \sim \mathbf{k}^2$ and the contact interaction $U_{\mathbf{q}} = \text{const} = U_0$:

$$\hat{H}_{\text{int,pair}} = U_0 \sum_{\mathbf{1234}} \hat{a}_1^\dagger \hat{a}_2^\dagger \hat{a}_3 \hat{a}_4 \delta_{\mathbf{1+2,3+4}}$$

First of all, we note that due to Kronecker delta $\delta_{\mathbf{1+2,3+4}}$, the expressions (9), (10) have the form of a discrete convolution

$$\sum_{k'=1}^L f(k')g(k-k') \equiv (f * g)(k), \quad (11)$$

which can be efficiently calculated using the Convolution Theorem:

$$(f * g)(k) = \frac{1}{L} \text{FFT}^{-1} [F(r) \cdot G(r)](k), \quad (12)$$

where $F(r)$, $G(r)$ are the Fourier transforms of functions $f(k)$, $g(k)$. This allows us to calculate the sum of (11)

with $\sim L \ln L$ operations using the Fast Fourier transform (FFT). In the case of a space of dimension d , the number of operations is $\sim V \ln V \sim L^d \ln L$.

Second, the same transformation can be performed on the energy axis, since the discrete particle energies in this model are proportional to integer numbers: $\varepsilon_n = n\varepsilon_1$, where $n = 0 \dots N_\varepsilon - 1$.

To correctly use this scheme for non-periodic functions, the extended range of values $n = 0 \dots N_{\text{max}} - 1$ is employed, with the so-called 'zero-padding' [25] at $n \geq N_\varepsilon$.

Finally, we introduce functions in the extended space $(\mathbf{k}, \varepsilon) \equiv \rho$ and $(\mathbf{r}, \gamma) \equiv \mathbf{R}$:

$$n_{\mathbf{k}\varepsilon} \equiv n_{\mathbf{k}} \delta_{\varepsilon, \varepsilon_{\mathbf{k}}}, \quad (13)$$

$$s_{\mathbf{k}\varepsilon} \equiv \delta_{\varepsilon, \varepsilon_{\mathbf{k}}}, \quad (14)$$

$$N_{\mathbf{R}} \equiv \text{FFT}(n_\rho), \quad (15)$$

$$S_{\mathbf{R}} \equiv \text{FFT}(s_\rho). \quad (16)$$

Substituting them in the expressions (9), (10) and replacing Kronecker delta symbols with sums $\delta_{\Delta\mathbf{k},0} = \frac{1}{L^3} \sum_{\mathbf{r}} e^{i\Delta\mathbf{k}\mathbf{r}}$ and $\delta_{\Delta\varepsilon,0} = \frac{1}{N_\varepsilon} \sum_{\gamma} e^{i\Delta\varepsilon\gamma}$, we obtain the final equation (the detailed derivation is given in Appendix):

$$\frac{dn_{\mathbf{k}}}{dt} = U_0^2 ([p_{\mathbf{k},\varepsilon_{\mathbf{k}}} + \tilde{p}_{2\mathbf{k},2\varepsilon_{\mathbf{k}}}] + n_{\mathbf{k}}[q_{\mathbf{k},\varepsilon_{\mathbf{k}}} + \tilde{q}_{2\mathbf{k},2\varepsilon_{\mathbf{k}}}]), \quad (17)$$

where

$$p_\rho \equiv \text{FFT}^{-1}(P_{\mathbf{R}}), \quad (18)$$

$$q_\rho \equiv \text{FFT}^{-1}(Q_{\mathbf{R}}),$$

$$\tilde{p}_\rho \equiv \text{FFT}^{-1}(\tilde{P}_{\mathbf{R}}),$$

$$\tilde{q}_\rho \equiv \text{FFT}^{-1}(\tilde{Q}_{\mathbf{R}}).$$

The four-dimensional matrices P , Q , \tilde{P} , \tilde{Q} in the case of Bose statistics are given by the expressions:

$$P_{\mathbf{R}} = S_{-\mathbf{R}} N_{\mathbf{R}}^2 + N_{-\mathbf{R}} N_{\mathbf{R}}^2 - N_{-\mathbf{R}} N_{2\mathbf{R}} - S_{-\mathbf{R}} N_{2\mathbf{R}} - N_{\mathbf{R}} \mathbb{Z}_{\mathbf{R}}, \quad (19)$$

$$\tilde{P}_{\mathbf{R}} = N_{\mathbf{R}}^2,$$

$$Q_{\mathbf{R}} = S_{-\mathbf{R}} n_{\mathbf{R}}^2 - 2N_{-\mathbf{R}} N_{\mathbf{R}} S_{\mathbf{R}} - N_{-\mathbf{R}} S_{\mathbf{R}}^2 - N_{-\mathbf{R}} S_{2\mathbf{R}} - S_{-\mathbf{R}} N_{2\mathbf{R}} - 2N_{-\mathbf{R}} N_{2\mathbf{R}} + S_{\mathbf{R}} \mathbb{Z}_{\mathbf{R}},$$

$$\tilde{Q}_{\mathbf{R}} = S_{\mathbf{R}}^2 + 2N_{\mathbf{R}} S_{\mathbf{R}} + 2N_{\mathbf{R}}^2.$$

and in the case of Fermi statistics (paying additional attention to spin indices):

$$\begin{aligned}
P_{\mathbf{R}} &= S_{-\mathbf{R}}N_{\mathbf{R}}^2 - N_{-\mathbf{R}}N_{\mathbf{R}}^2 + N_{-\mathbf{R}}N_{2\mathbf{R}} - S_{-\mathbf{R}}N_{2\mathbf{R}} + N_{\mathbf{R}}Z_{\mathbf{R}}, \\
\tilde{P}_{\mathbf{R}} &= -N_{\mathbf{R}}^2, \\
Q_{\mathbf{R}} &= -S_{-\mathbf{R}}N_{\mathbf{R}}^2 + 2N_{-\mathbf{R}}N_{\mathbf{R}}S_{\mathbf{R}} - N_{-\mathbf{R}}S_{\mathbf{R}}^2 + N_{-\mathbf{R}}S_{2\mathbf{R}} + S_{-\mathbf{R}}N_{2\mathbf{R}} - 2N_{-\mathbf{R}}N_{2\mathbf{R}} - S_{\mathbf{R}}Z_{\mathbf{R}}, \\
\tilde{Q}_{\mathbf{R}} &= S_{\mathbf{R}}^2 - 2N_{\mathbf{R}}S_{\mathbf{R}} + 2N_{\mathbf{R}}^2.
\end{aligned} \tag{20}$$

The function $Z_{\mathbf{R}}$ is defined in Appendix.

As we see, multiple sums in the expressions (9), (10) are converted to several more performance-efficient Fourier transforms. The achieved reduction in the amount of calculations makes it possible to increase the available size of the system to a relatively macroscopic $L \sim 16 \div 48$. Later in the Chapter III, we show the application of this method to the detailed study of relaxation times in weakly interacting Bose and Fermi systems.

Note that more complex models with momentum-dependent interaction $U_{\mathbf{q}} \neq \text{const}$ can also use this transformation in almost identical way but the expressions are slightly more complicated. For example, the second term in the Eq. (19) takes the form:

$$U_0^2 n_{-\mathbf{R}} n_{\mathbf{R}}^2 \rightarrow N_{\mathbf{r}\gamma} \cdot \sum_{\mathbf{r}'} N_{\mathbf{r}',-\gamma} N_{-\mathbf{r}',\gamma} u_{\mathbf{r}+\mathbf{r}} \tag{21}$$

where $u_{\mathbf{r}} \equiv \text{FFT}(U_{\mathbf{q}}^2)$. The sum can again be recognized as a convolution and calculated with appropriate sequence of Fourier transforms.

d. The generalization to arbitrary energy levels.

Now we show how to extend this approach to the case of arbitrary energy levels $\varepsilon_{\mathbf{k}}$, i.e. for systems with non-parabolic dispersion law (electrons far from the band edge, exciton polaritons, Bogoliubov quasiparticles, etc.). If the discrete energy levels are not proportional to integer numbers, the precise Fourier transform on the energy axis used in transformation (19), (20) is not possible.

Using the smaller step on the energy axis we can make the grid values closer to the actual single-particle energy levels. The necessary accuracy of the approximation is determined by the width of the levels in the physical problem.

In the equations (9), (10) we replace $\delta_{\Delta\varepsilon,0}$ to broadening factor $f(\varepsilon_1 + \varepsilon_2 - \varepsilon_3 - \varepsilon_4)$, which describes the accuracy of the energy conservation. Depending on the problem under consideration, it can be taken in the form of Lorentzian or Gaussian function [26]. The introducing of the broadening factor alongwith the reasonable choice of smaller energy step allow us to consider systems with an arbitrary not equidistant single-particle spectrum.

We can notice that typical terms that have received the additional multiplier (broadening factor) can still be represented by multiple convolution:

$$\sum_{\substack{\mathbf{k}_2 \mathbf{k}_3 \mathbf{k}_4 \\ \varepsilon_2 \varepsilon_3 \varepsilon_4}} (\dots) \delta_{\Delta\varepsilon,0} \rightarrow \sum_{\substack{\mathbf{k}_2 \mathbf{k}_3 \mathbf{k}_4 \\ \varepsilon_2 \varepsilon_3 \varepsilon_4}} (\dots) f(\Delta\varepsilon). \tag{22}$$

As a result, the expressions in (18) become

$$\begin{aligned}
p_{\mathbf{k}\varepsilon} &\equiv \text{FFT}^{-1}(P_{\mathbf{r}\gamma} F(\gamma)), \\
q_{\mathbf{k}\varepsilon} &\equiv \text{FFT}^{-1}(Q_{\mathbf{r}\gamma} F(\gamma)), \\
\tilde{p}_{\mathbf{k}\varepsilon} &\equiv \text{FFT}^{-1}(\tilde{P}_{\mathbf{r}\gamma} F(\gamma)), \\
\tilde{q}_{\mathbf{k}\varepsilon} &\equiv \text{FFT}^{-1}(\tilde{Q}_{\mathbf{r}\gamma} F(\gamma)),
\end{aligned} \tag{23}$$

where $F(\gamma)$ is the Fourier transform of the factor $f(\varepsilon)$.

To verify the correctness of the transformation, the results of calculation using Eqs.(17)–(23) were compared with the direct summation of the original expressions (9), (10) for several small systems with dimensions $4 \times 4 \times 4$, $8 \times 8 \times 8$ and various particle statistics. The resulting numbers were equal with the precision of at least 13 digits for all the problem parameters, proving the validity of the presented method.

As a conclusion, in this Chapter we reported the universal approach for numerical simulation of the kinetics in interacting quantum system with arbitrary energy spectrum on a finite momentum lattice of relatively large dimensions.

III. RELAXATION TIME IN FINITE FERMI AND BOSE SYSTEMS

Generally, the study of kinetics by numerical solution of equations (5),(9),(10) is quite laborous. For problems with occupation numbers near the equilibrium $n_{\mathbf{k}} \simeq n_{\mathbf{k}}^{(0)} \equiv f(\varepsilon_{\mathbf{k}}, \mu, T)$, a simple model based on characteristic relaxation times is often used:

$$\frac{dn_{\mathbf{k}}}{dt} = -\frac{1}{\tau_{\mathbf{k}}} (n_{\mathbf{k}} - n_{\mathbf{k}}^{(0)}). \tag{24}$$

Values of $\tau_{\mathbf{k}}$ are estimated from existing analytical expressions or experimental data.

There exists a well-known expression in the Fermi-liquid theory [4] for the lifetime of quasiparticles near Fermi surface:

$$\tau(\varepsilon) \sim \frac{1}{(\pi k_B T)^2 + (\varepsilon - F)^2}, \tag{25}$$

where F is the Fermi level.

For the Bose gas, analytical results for lifetime of quasiparticles in some limit cases are available, namely, the so-called Beliaev damping [27, 28] and Landau damping [28, 29].

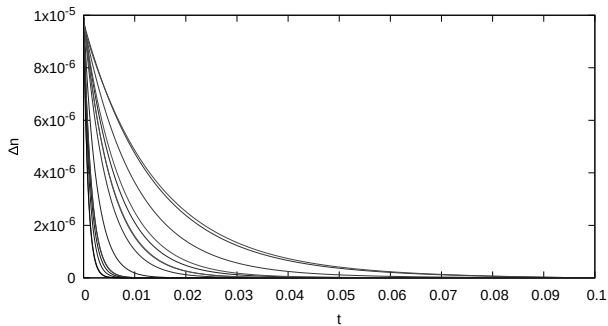


Figure 2: Relaxation of nonequilibrium occupation $\Delta n_{\mathbf{k}}(t)$ for Fermi gas on the lattice $8 \times 8 \times 8$, Fermi energy $F = 2.0$, Fermi surface radius $k_F = \pi/2a$.

Detailed data on the momentum dependency of characteristic times $\tau_{\mathbf{k}}$ would make it possible to improve the quality of model (24). Using numerical calculation with the method reported in Chapter II, we can obtain the values of relaxation times for the complete range of momenta in the system. In this Chapter, we present the calculation details and the results for relaxation times of weakly interacting Fermi and Bose gases on a finite momentum lattice.

a. Calculation details. In order to determine the momentum dependency of relaxation time $\tau_{\mathbf{k}}$, the evolution of the equilibrium system excited at the corresponding momenta was simulated. The excitation at the given momentum \mathbf{k} was done by increasing the occupation number $n_{\mathbf{k}}$ by a small value $\Delta n_{\mathbf{k}}(t=0) \sim 10^{-3}$.

The typical time dependency of nonequilibrium occupations $\Delta n_{\mathbf{k}}(t)$ demonstrating the exponential-like decay is shown in Figure 2. The dependency $\Delta n_{\mathbf{k}}(t) = Ae^{-t/\tau_{\mathbf{k}}}$ allows to use the relation for the relaxation time

$$\tau_{\mathbf{k}} = -\frac{dn_{\mathbf{k}}/dt}{d^2n_{\mathbf{k}}/dt^2}, \quad (26)$$

where the derivatives are calculated using a finite-difference scheme.

The scale of relaxation time is determined by energy units. In this Chapter, we put $U_0 = 1$.

b. Relaxation time in Fermi gas. First we calculate the relaxation times $\tau_{\mathbf{k}}$ in the weakly interacting Fermi gas where analytical result (25) exists, so that the verification of the simulation method can be made.

The Hamiltonian of the system is:

$$\hat{H} = \sum_{\mathbf{k}\sigma} \varepsilon_{\mathbf{k}} \hat{n}_{\mathbf{k}\sigma} + U_0 \sum_{\mathbf{k}\mathbf{p}\mathbf{q}} \hat{a}_{\mathbf{k}\uparrow}^\dagger \hat{a}_{\mathbf{p}\downarrow}^\dagger \hat{a}_{\mathbf{p}+\mathbf{q}\downarrow} \hat{a}_{\mathbf{k}-\mathbf{q}\uparrow}, \quad (27)$$

where $\varepsilon_{\mathbf{k}} = \frac{\varepsilon_1}{\Delta k^2} \mathbf{k}^2$, $\Delta k = \frac{2\pi}{La}$ is the discreteness of the momentum in the Brillouin zone, determined by the size of the crystal.

In the Figures 3, 4 the calculated relaxation time is shown as a function of momentum for the Fermi system at several temperatures $k_B T = 0.2, 0.3, 0.5, 0.7, 1.0$.

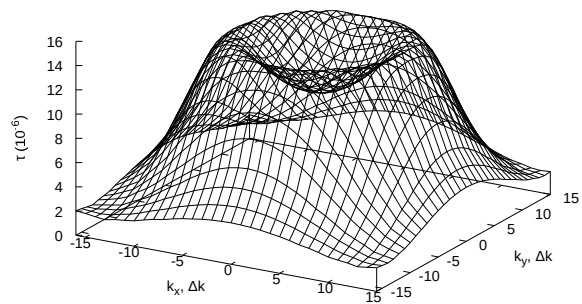


Figure 3: Relaxation time $\tau_{\mathbf{k}}$ calculated for the Fermi gas on the lattice $32 \times 32 \times 32$, $F = 2.0$, $k_F = \pi/2a$, $k_B T = 0.7$, as a function of momentum $\mathbf{k} = (k_x, k_y, 0)$.

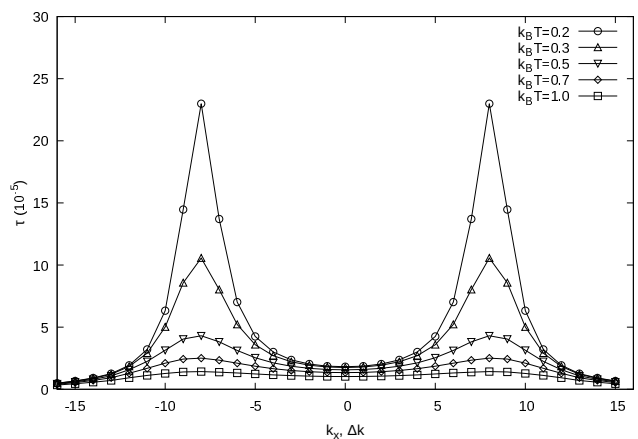


Figure 4: Relaxation time as a function of momentum $\mathbf{k} = (k_x, 0, 0)$, calculated for the Fermi gas on the lattice $32 \times 32 \times 32$, $F = 2.0$, $k_F = \pi/2a$, for several temperatures. Lines are to guide the eye.

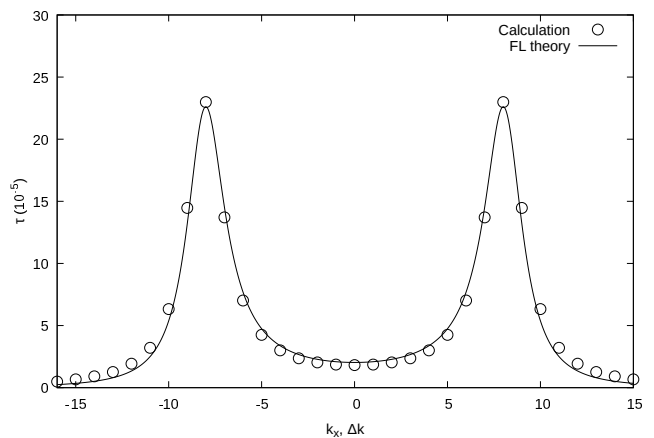


Figure 5: The calculated relaxation time compared with the Fermi-liquid theory, Eq. (25). The parameters of the system are the same as for Figure 4, temperature $k_B T = 0.2$.

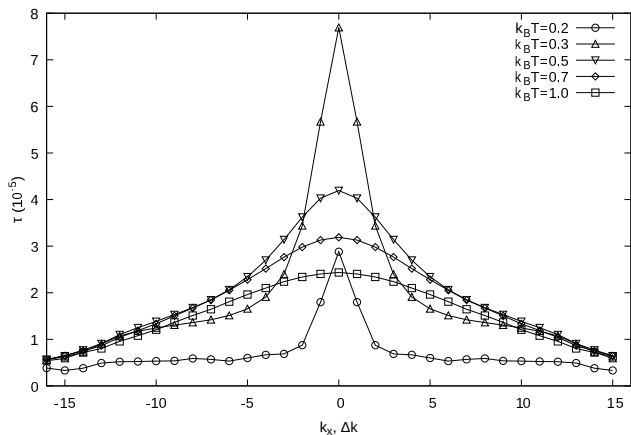


Figure 6: Relaxation time as a function of momentum $\mathbf{k} = (k_x, 0, 0)$, calculated for the Bose gas on the lattice $32 \times 32 \times 32$, with total particle number $N = 10^3$, for several temperatures $k_B T = 0.2, 0.3, 0.5, 0.7, 1.0$.

We see the typical Fermi-liquid behaviour reaching maximum values near the Fermi surface and proportional to T^{-2} . To demonstrate the overall agreement with the theory, the values calculated for temperature $k_B T = 0.2$ are shown in the Figure 5 alongwith the analytical dependence (25).

We can conclude that the application of the reported method allows to calculate the momentum dependency of the relaxation time in the weakly interacting quantum gases.

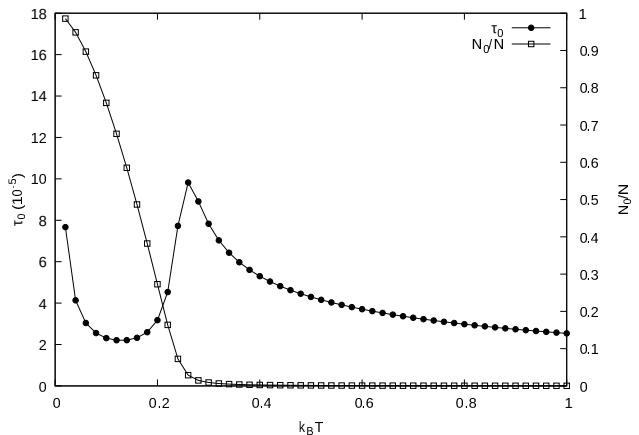
c. Relaxation time in Bose gas. Next we apply this approach to the weakly interacting Bose gas. The Hamiltonian is

$$\hat{H} = \sum_{\mathbf{k}} \varepsilon_{\mathbf{k}} \hat{n}_{\mathbf{k}} + U_0 \sum_{\mathbf{k}, \mathbf{p}, \mathbf{q}} \hat{a}_{\mathbf{k}}^\dagger \hat{a}_{\mathbf{p}}^\dagger \hat{a}_{\mathbf{p}+\mathbf{q}} \hat{a}_{\mathbf{k}-\mathbf{q}}. \quad (28)$$

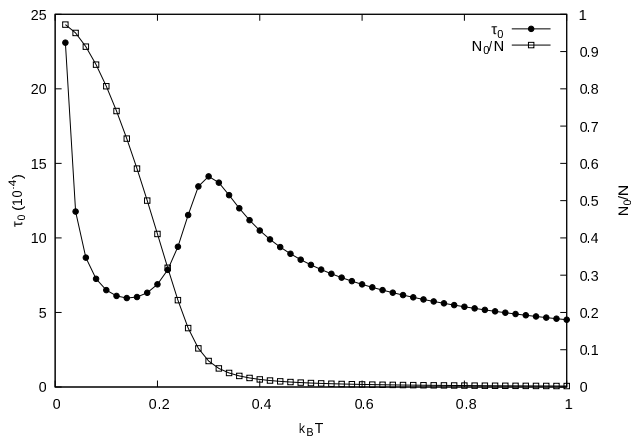
The calculated relaxation times as a function of momentum for Bose system with the total particle number $N=10^3$ is shown in Figure 6. We see that the relaxation becomes slower as the energy $\varepsilon_{\mathbf{k}}$ decreases.

The temperature dependency of the relaxation time τ_0 at the central momentum $\mathbf{k} = 0$ is given in Figure 7 (a). The parameters of the problem were chosen such that the Bose-Einstein condensation occurs at high enough temperature ($T_c=0.2236$). The dependence $\tau_0(T)$ shows the pronounced peak near the transition point. At low temperatures the second feature is visible. We associate it to the increasing difficulty of the energy transfer to the discrete spectrum caused by the finite momentum lattice.

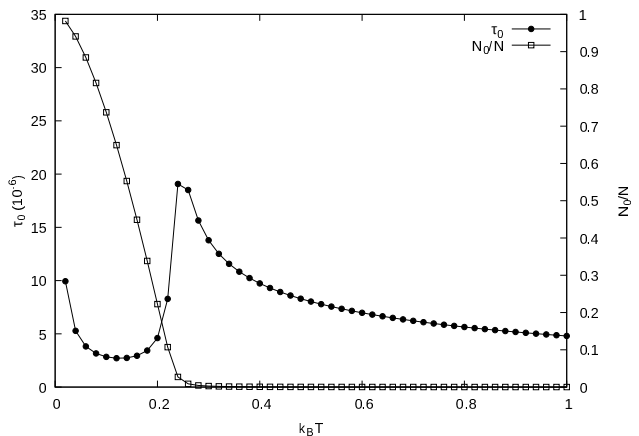
To reveal the effect of lattice size, we performed the calculations for different sizes $L=16, 48$ with the same particle density ($N=125, 3375$, correspondingly). The functions $\tau_0(T)$ are shown in Figures 7 (b) and (c). As we see, the low temperature feature in relaxation time becomes relatively weaker with increasing system size, while



(a)



(b)



(c)

Figure 7: Relaxation time in Bose gas for momentum $\mathbf{k} = 0$ as a function of temperature, calculated for various lattice sizes $L=32$ (a), 16 (b), 48 (c), with the particle density large enough to show the BEC transition (total particle number $N=1000, 125, 3375$, correspondingly). For reference, the occupation $N_0(T)$ is plotted.

the qualitative behaviour at large temperatures $T \gtrsim T_c$ remains almost the same with minor change of the peak sharpness as the phase transition becomes narrower.

IV. CONCLUSION

We presented a universal and efficient method for numerical simulation of kinetics of weakly interacting quantum systems on a finite momentum lattice, using the original transformation to improve the efficiency and to increase the affordable system sizes. This approach can be applied to the wide range of models of various statistics with arbitrary single-particle spectrum $\varepsilon_{\mathbf{q}}$ and two-particle interaction obeying the momentum conservation. The system size can be as large as $\sim 50^3$, which can help to obtain properties of continual systems using appropriate extrapolation.

As a demonstration, the momentum dependence of relaxation time was calculated for the weakly interacting Fermi gas on the momentum lattice $32 \times 32 \times 32$, in overall agreement with Fermi-liquid theory predictions (Figure 5). Similar calculation for weakly interacting Bose gas shows the temperature dependence with features near to

the BEC transition point and at low temperatures due to discrete energy spectrum (Figure 7).

The numerical method reported in this article can be applied to various time-dependent problems, such as relaxation processes in superconductors, behaviour of nonequilibrium carriers in semiconductors [21] and metals [30], kinetics of atomic gases in magneto-optical traps [31], *etc.*

Acknowledgments

The work was supported by the Ministry of Science and Higher Education of Russian Federation (state assignment project No. 0723-2020-0036).

Appendix A: Appendix: Transformation

In this Appendix, we show how to convert equations (9), (10) to (17), (19), (20) in the case of Bose statistics. First, we expand the brackets in the equation (9):

$$\begin{aligned} \frac{dn_{\mathbf{k}_1}}{dt} = U_0^2 \sum_{\mathbf{k}_2 \mathbf{k}_3 \mathbf{k}_4} \{ & [n_2 n_3 n_4 + n_3 n_4 + n_1 (n_3 n_4 - n_2 n_3 - n_2 n_4 - n_2) \\ & - \delta_{34} [(n_2 n_3 + n_3) + n_1 (2n_2 n_3 + n_2 + n_3)] \\ & + \delta_{12} [n_3 n_4 + n_1 (2n_3 n_4 + n_3 + n_4 + 1)] \\ & + \delta_{12} \delta_{34} (n_1 - n_3) \} \delta_{\varepsilon_1 + \varepsilon_2, \varepsilon_3 + \varepsilon_4} \delta_{\mathbf{1} + \mathbf{2}, \mathbf{3} + \mathbf{4}} \end{aligned} \quad (\text{A1})$$

Here we grouped the terms where the particle momenta coincide in the initial or final states (δ_{12} and δ_{34} , correspondingly).

a. The first line in the expression (A1) can be conveniently written as:

$$\left(\frac{dn_{\mathbf{k}_1}}{dt} \right)^{(1)} = U_0^2 [(A_{\mathbf{k}_1} + B_{\mathbf{k}_1}) + n_{\mathbf{k}_1} (B_{\mathbf{k}_1} - 2C_{\mathbf{k}_1} - D_{\mathbf{k}_1})], \quad (\text{A2})$$

where

$$A_{\mathbf{k}_1} \equiv \sum_{\mathbf{k}_2 \mathbf{k}_3 \mathbf{k}_4} n_{\mathbf{k}_2} n_{\mathbf{k}_3} n_{\mathbf{k}_4} \delta_{\varepsilon_1 + \varepsilon_2, \varepsilon_3 + \varepsilon_4} \delta_{\mathbf{k}_1 + \mathbf{k}_2, \mathbf{k}_3 + \mathbf{k}_4}, \quad (\text{A3})$$

$$B_{\mathbf{k}_1} \equiv \sum_{\mathbf{k}_2 \mathbf{k}_3 \mathbf{k}_4} n_{\mathbf{k}_3} n_{\mathbf{k}_4} \delta_{\varepsilon_1 + \varepsilon_2, \varepsilon_3 + \varepsilon_4} \delta_{\mathbf{k}_1 + \mathbf{k}_2, \mathbf{k}_3 + \mathbf{k}_4}, \quad (\text{A4})$$

$$C_{\mathbf{k}_1} \equiv \sum_{\mathbf{k}_2 \mathbf{k}_3 \mathbf{k}_4} n_{\mathbf{k}_2} n_{\mathbf{k}_3} \delta_{\varepsilon_1 + \varepsilon_2, \varepsilon_3 + \varepsilon_4} \delta_{\mathbf{k}_1 + \mathbf{k}_2, \mathbf{k}_3 + \mathbf{k}_4}, \quad (\text{A5})$$

$$D_{\mathbf{k}_1} \equiv \sum_{\mathbf{k}_2 \mathbf{k}_3 \mathbf{k}_4} n_{\mathbf{k}_2} \delta_{\varepsilon_1 + \varepsilon_2, \varepsilon_3 + \varepsilon_4} \delta_{\mathbf{k}_1 + \mathbf{k}_2, \mathbf{k}_3 + \mathbf{k}_4}. \quad (\text{A6})$$

We rewrite the expression (A3) in the expanded space

$(\mathbf{k}, \varepsilon) \equiv \rho$, employ the notation (13)-(16), and replace Kronecker delta symbols with sums:

$$\begin{aligned} A_{\mathbf{k}_1 \varepsilon_1} &= \frac{1}{L^3 N_\varepsilon} \sum_{\substack{\mathbf{k}_2 \mathbf{k}_3 \mathbf{k}_4 \\ \varepsilon_2 \varepsilon_3 \varepsilon_4}} n_{\mathbf{k}_2 \varepsilon_2} n_{\mathbf{k}_3 \varepsilon_3} n_{\mathbf{k}_4 \varepsilon_4} \\ &\times \sum_{\mathbf{r} \gamma} e^{i(\mathbf{k}_1 + \mathbf{k}_2 - \mathbf{k}_3 - \mathbf{k}_4) \mathbf{r}} e^{i(\varepsilon_1 + \varepsilon_2 - \varepsilon_3 - \varepsilon_4) \gamma} \end{aligned} \quad (\text{A7})$$

Using the relation $n_{\mathbf{k} \varepsilon} = \sum_{\mathbf{r} \gamma} N_{\mathbf{r} \gamma} e^{i(\mathbf{k} \mathbf{r} + \varepsilon \gamma)}$, we can write:

$$\begin{aligned} A_{\mathbf{k}_1 \varepsilon_1} &= \frac{1}{L^3 N_\varepsilon} \sum_{\substack{\mathbf{k}_2 \mathbf{k}_3 \mathbf{k}_4 \\ \varepsilon_2 \varepsilon_3 \varepsilon_4}} \sum_{\substack{\mathbf{r}_2 \mathbf{r}_3 \mathbf{r}_4 \\ \gamma_2 \gamma_3 \gamma_4}} N_{\mathbf{r}_2 \gamma_2} N_{\mathbf{r}_3 \gamma_3} N_{\mathbf{r}_4 \gamma_4} \\ &\times \sum_{\mathbf{r} \gamma} e^{i(\mathbf{k}_2 \mathbf{r}_2 + \mathbf{k}_3 \mathbf{r}_3 + \mathbf{k}_4 \mathbf{r}_4)} e^{i(\varepsilon_2 \gamma_2 + \varepsilon_3 \gamma_3 + \varepsilon_4 \gamma_4)} \\ &\times e^{i(\mathbf{k}_1 + \mathbf{k}_2 - \mathbf{k}_3 - \mathbf{k}_4) \mathbf{r}} e^{i(\varepsilon_1 + \varepsilon_2 - \varepsilon_3 - \varepsilon_4) \gamma} \\ &= \frac{1}{L^3 N_\varepsilon} \sum_{\mathbf{r} \gamma} N_{-\mathbf{r}, -\gamma} N_{\mathbf{r} \gamma} N_{\mathbf{r} \gamma} e^{i(\mathbf{k}_1 \mathbf{r} + \varepsilon_1 \gamma)}, \end{aligned} \quad (\text{A8})$$

which takes in the form of the Fourier transform.

The functions B , C , D can be converted in the same way. As a result, we obtain:

$$A_{\mathbf{r}\gamma} = N_{-\mathbf{r},-\gamma}(N_{\mathbf{r}\gamma})^2, \quad (\text{A9})$$

$$B_{\mathbf{r}\gamma} = S_{-\mathbf{r},-\gamma}(N_{\mathbf{r}\gamma})^2, \quad (\text{A10})$$

$$C_{\mathbf{r}\gamma} = N_{-\mathbf{r},-\gamma}N_{\mathbf{r}\gamma}S_{\mathbf{r}\gamma}, \quad (\text{A11})$$

$$D_{\mathbf{r}\gamma} = N_{-\mathbf{r},-\gamma}(S_{\mathbf{r}\gamma})^2, \quad (\text{A12})$$

where $S_{\mathbf{r}\gamma}$ is the Fourier transform of the previously in-

roduced function $s_{\mathbf{k}\varepsilon} \equiv \delta_{\varepsilon,\varepsilon_{\mathbf{k}}}$.

The function $A_{\mathbf{r}\gamma}, \dots, D_{\mathbf{r}\gamma}$ are turned into $A_{\mathbf{k}\varepsilon}, \dots, D_{\mathbf{k}\varepsilon}$ using the inverse Fourier transform, after that the desired values $A_{\mathbf{k}}, \dots, D_{\mathbf{k}}$ for the expression (A2) can be obtained with $\varepsilon = \varepsilon_{\mathbf{k}}$.

b. The second line in the expression (A1) corresponds to the case when $\mathbf{k}_3 = \mathbf{k}_4$. It can be written as:

$$\left(\frac{dn_{\mathbf{k}_1}}{dt}\right)^{(2)} = -U_0^2 [(E_{\mathbf{k}_1} + F_{\mathbf{k}_1}) + n_{\mathbf{k}_1}(2E_{\mathbf{k}_1} + F_{\mathbf{k}_1} + G_{\mathbf{k}_1})], \quad (\text{A13})$$

where

$$E_{\mathbf{k}_1} \equiv \sum_{\mathbf{k}_2\mathbf{k}_3\mathbf{k}_4} n_{\mathbf{k}_2}n_{\mathbf{k}_3}\delta_{\mathbf{k}_3,\mathbf{k}_4}\delta_{\varepsilon_1+\varepsilon_2,\varepsilon_3+\varepsilon_4}\delta_{\mathbf{k}_1+\mathbf{k}_2,\mathbf{k}_3+\mathbf{k}_4}, \quad (\text{A14})$$

$$F_{\mathbf{k}_1} \equiv \sum_{\mathbf{k}_2\mathbf{k}_3\mathbf{k}_4} n_{\mathbf{k}_3}\delta_{\mathbf{k}_3,\mathbf{k}_4}\delta_{\varepsilon_1+\varepsilon_2,\varepsilon_3+\varepsilon_4}\delta_{\mathbf{k}_1+\mathbf{k}_2,\mathbf{k}_3+\mathbf{k}_4}, \quad (\text{A15})$$

$$G_{\mathbf{k}_1} \equiv \sum_{\mathbf{k}_2\mathbf{k}_3\mathbf{k}_4} n_{\mathbf{k}_2}\delta_{\mathbf{k}_3,\mathbf{k}_4}\delta_{\varepsilon_1+\varepsilon_2,\varepsilon_3+\varepsilon_4}\delta_{\mathbf{k}_1+\mathbf{k}_2,\mathbf{k}_3+\mathbf{k}_4}. \quad (\text{A16})$$

A reasoning similar to the previous paragraph gives the expressions:

$$E_{\mathbf{r}\gamma} = N_{-\mathbf{r},-\gamma}N_{2\mathbf{r}2\gamma}, \quad (\text{A17})$$

$$F_{\mathbf{r}\gamma} = S_{-\mathbf{r},-\gamma}N_{2\mathbf{r}2\gamma}, \quad (\text{A18})$$

$$G_{\mathbf{r}\gamma} = N_{-\mathbf{r},-\gamma}S_{2\mathbf{r}2\gamma}. \quad (\text{A19})$$

c. The third line in the expression (A1) corresponds to the case when $\mathbf{k}_1 = \mathbf{k}_2$. Taking into consideration the

same role of \mathbf{k}_3 and \mathbf{k}_4 in the sums, this line can be written as:

$$\left(\frac{dn_{\mathbf{k}_1}}{dt}\right)^{(3)} = U_0^2 [H_{\mathbf{k}_1} + n_{\mathbf{k}_1}(2H_{\mathbf{k}_1} + 2I_{\mathbf{k}_1} + J_{\mathbf{k}_1})], \quad (\text{A20})$$

where

$$H_{\mathbf{k}_1} \equiv \sum_{\mathbf{k}_2\mathbf{k}_3\mathbf{k}_4} n_{\mathbf{k}_3}n_{\mathbf{k}_4}\delta_{\mathbf{k}_1,\mathbf{k}_2}\delta_{\varepsilon_1+\varepsilon_2,\varepsilon_3+\varepsilon_4}\delta_{\mathbf{k}_1+\mathbf{k}_2,\mathbf{k}_3+\mathbf{k}_4}, \quad (\text{A21})$$

$$I_{\mathbf{k}_1} \equiv \sum_{\mathbf{k}_2\mathbf{k}_3\mathbf{k}_4} n_{\mathbf{k}_3}\delta_{\mathbf{k}_1,\mathbf{k}_2}\delta_{\varepsilon_1+\varepsilon_2,\varepsilon_3+\varepsilon_4}\delta_{\mathbf{k}_1+\mathbf{k}_2,\mathbf{k}_3+\mathbf{k}_4}, \quad (\text{A22})$$

$$J_{\mathbf{k}_1} \equiv \sum_{\mathbf{k}_2\mathbf{k}_3\mathbf{k}_4} \delta_{\mathbf{k}_1,\mathbf{k}_2}\delta_{\varepsilon_1+\varepsilon_2,\varepsilon_3+\varepsilon_4}\delta_{\mathbf{k}_1+\mathbf{k}_2,\mathbf{k}_3+\mathbf{k}_4}. \quad (\text{A23})$$

Repeating the transformation made in (A7), we convert the equation (A21) to the form:

$$H_{\mathbf{k}_1\varepsilon_1} = \frac{1}{L^3 N_\varepsilon} \sum_{\mathbf{r}\gamma} N_{\mathbf{r}\gamma} N_{\mathbf{r}\gamma} e^{i(2\mathbf{k}_1\mathbf{r}+2\varepsilon_1\gamma)} = \tilde{H}_{2\mathbf{k}_1,2\varepsilon_1} \quad (\text{A24})$$

i.e. the required values of $H_{\mathbf{k}_1\varepsilon_1}$ are calculated using the Fourier transform of the auxiliary function

$$\tilde{H}_{\mathbf{r}\gamma} = (N_{\mathbf{r}\gamma})^2. \quad (\text{A25})$$

The auxiliary functions for variables $I_{\mathbf{k}_1\varepsilon_1}$ and $J_{\mathbf{k}_1\varepsilon_1}$

are obtained similarly:

$$\tilde{I}_{\mathbf{r}\gamma} = N_{\mathbf{r}\gamma} S_{\mathbf{r}\gamma}, \quad (\text{A26})$$

$$\tilde{J}_{\mathbf{r}\gamma} = (S_{\mathbf{r}\gamma})^2. \quad (\text{A27})$$

d. The fourth line in the expression (A1) corresponds to the case when $\mathbf{k}_1 = \mathbf{k}_2$ and $\mathbf{k}_3 = \mathbf{k}_4$. It can be

written as:

$$\left(\frac{dn_{\mathbf{k}_1}}{dt} \right)^{(4)} = U_0^2 [-X_{\mathbf{k}_1} + n_{\mathbf{k}_1} Y_{\mathbf{k}_1}], \quad (\text{A28})$$

where

$$X_{\mathbf{k}_1} \equiv \sum_{\mathbf{k}_2 \mathbf{k}_3 \mathbf{k}_4} n_{\mathbf{k}_3} \delta_{\mathbf{k}_1, \mathbf{k}_2} \delta_{\mathbf{k}_3, \mathbf{k}_4} \delta_{\varepsilon_1 + \varepsilon_2, \varepsilon_3 + \varepsilon_4} \delta_{\mathbf{k}_1 + \mathbf{k}_2, \mathbf{k}_3 + \mathbf{k}_4}, \quad (\text{A29})$$

$$Y_{\mathbf{k}_1} \equiv \sum_{\mathbf{k}_2 \mathbf{k}_3 \mathbf{k}_4} \delta_{\mathbf{k}_1, \mathbf{k}_2} \delta_{\mathbf{k}_3, \mathbf{k}_4} \delta_{\varepsilon_1 + \varepsilon_2, \varepsilon_3 + \varepsilon_4} \delta_{\mathbf{k}_1 + \mathbf{k}_2, \mathbf{k}_3 + \mathbf{k}_4}. \quad (\text{A30})$$

Taking into consideration the equalities $\mathbf{k}_1 = \mathbf{k}_2$, $\mathbf{k}_3 = \mathbf{k}_4$, the relation $\mathbf{k}_1 + \mathbf{k}_2 = \mathbf{k}_3 + \mathbf{k}_4$ can be rewritten as $2\mathbf{k}_1 = 2\mathbf{k}_3 + \mathbb{G}$. It means that the momenta \mathbf{k}_1 and \mathbf{k}_3 are either equal or differ by a half of the unit vector of the reciprocal lattice. To obtain all different vectors \mathbf{k}_3 for a given \mathbf{k}_1 , we should use all half-vectors of reciprocal lattice (including zero vector) contained in the first Brillouin zone. We denote them as $\mathbb{G}/2$.

In this case, we get the expressions similar to (A8) with extra factor $e^{i(\mathbf{k}_1 - \mathbf{k}_3)\mathbf{r}} = e^{i\mathbf{r}\mathbb{G}/2}$:

$$X_{\mathbf{k}_1 \varepsilon_1} = \frac{1}{L^3 N_\varepsilon} \sum_{\mathbf{r}\gamma} e^{i(\mathbf{k}_1 \mathbf{r} + \varepsilon_1 \gamma)} N_{\mathbf{r}\gamma} \sum_{\mathbb{G}/2} e^{i\mathbf{r}\mathbb{G}/2}, \quad (\text{A31})$$

$$Y_{\mathbf{k}_1 \varepsilon_1} = \frac{1}{L^3 N_\varepsilon} \sum_{\mathbf{r}\gamma} e^{i(\mathbf{k}_1 \mathbf{r} + \varepsilon_1 \gamma)} S_{\mathbf{r}\gamma} \sum_{\mathbb{G}/2} e^{i\mathbf{r}\mathbb{G}/2}. \quad (\text{A32})$$

The factor $\sum_{\mathbb{G}/2} e^{i\mathbf{r}\mathbb{G}/2} \equiv \mathbb{Z}_{\mathbf{r}}$ contains 2^d terms (where d is the dimension of space) and is equal to either 0 or 2^d , depending on the components of the vector \mathbf{r} .

As a result, we obtain:

$$\tilde{X}_{\mathbf{r}\gamma} = N_{\mathbf{r}\gamma} \mathbb{Z}_{\mathbf{r}}, \quad (\text{A33})$$

$$\tilde{Y}_{\mathbf{r}\gamma} = S_{\mathbf{r}\gamma} \mathbb{Z}_{\mathbf{r}}. \quad (\text{A34})$$

The relations for Fermi statistics are derived using the same reasoning. Combining all the terms $A_{\mathbf{r}\gamma}, \dots, Y_{\mathbf{r}\gamma}$, we get the expressions (19), (20).

-
- [1] E. Linaryd, M. Trushin, K. Watanabe, T. Taniguchi, and G. Eda, Electro-Optic Upconversion in van der Waals Heterostructures via Nonequilibrium Photocarrier Tunneling, *Adv. Mater.* **32**, 2001543 (2020).
- [2] I-Ju Chen, S. Limpert, W. Metaferia, C. Thelander, L. Samuelson, F. Capasso, A. M. Burke, and H. Linke, Hot-Carrier Extraction in Nanowire-Nanoantenna Photovoltaic Devices, *Nano Lett.* **20**, 4064 (2020).
- [3] B. Rethfeld, A. Kaiser, M. Vicanek, and G. Simon, Ultrafast dynamics of nonequilibrium electrons in metals under femtosecond laser irradiation, *Phys. Rev. B* **65**, 214303 (2002).
- [4] V. V. Kabanov and A. S. Alexandrov, Electron relaxation in metals: Theory and exact analytical solutions, *Phys. Rev. B* **78**, 174514 (2008).
- [5] R. M. Lutchyn, L. I. Glazman, and A. I. Larkin, Kinetics of the superconducting charge qubit in the presence of a quasiparticle, *Phys. Rev. B* **74**, 064515 (2006); **75**, 229903 (2007).
- [6] Yu. N. Ovchinnikov and V. Z. Kresin, Nonstationary state of superconductors: Application to nonequilibrium tunneling detectors, *Phys. Rev. B* **58**, 12416 (1998).
- [7] O. L. Berman, G. Gumbs, and R. Ya. Kezerashvili, Bose-Einstein condensation and superfluidity of dipolar excitons in a phosphorene double layer, *Phys. Rev. B* **96**, 014505 (2017).
- [8] L. F. Lastras-Martínez, E. Cerda-Méndez, N. Ulloa-Castillo, R. Herrera-Jasso, L. E. Rodríguez-Tapia, O. Ruiz-Cigarrillo, R. Castro-García, K. Biermann, and P. V. Santos, Microscopic optical anisotropy of exciton-polaritons in a GaAs-based semiconductor microcavity, *Phys. Rev. B* **96**, 235306 (2017).
- [9] M. R. Sturm, M. Schlosser, R. Walser, and G. Birkel, Quantum simulators by design: Many-body physics in reconfigurable arrays of tunnel-coupled traps, *Phys. Rev. A* **95**, 063625 (2017).
- [10] T. A. Schulze, T. Hartmann, K. K. Voges, M. W. Gempel, Feshbach spectroscopy and dual-species Bose-Einstein condensation of ^{23}Na - ^{39}K mixtures, *Phys. Rev. A* **97**, 023623 (2018).
- [11] N. G. Berloff and B. V. Svistunov, Scenario of strongly nonequilibrated Bose-Einstein condensation, *Phys. Rev. A* **66**, 013603 (2002).
- [12] L. Banyai and P. Gartner, Real-Time Bose-Einstein Condensation in a Finite Volume with a Discrete Spectrum, *Phys. Rev. Lett.* **88**, 210404 (2002).

- [13] C. J. E. Straatsma, V. E. Colussi, M. J. Davis, D. S. Lober, M. J. Holland, D. Z. Anderson, H. J. Lewandowski, and E. A. Cornell, Collapse and revival of the monopole mode of a degenerate Bose gas in an isotropic harmonic trap, *Phys. Rev. A* **94**, 043640 (2016).
- [14] V. V. Kabanov, J. Demsar, and D. Mihailovic, Kinetics of a Superconductor Excited with a Femtosecond Optical Pulse, *Phys. Rev. Lett.* **95**, 147002 (2005).
- [15] M. Wais, M. Eckstein, R. Fischer, P. Werner, M. Battiato, and K. Held, Quantum Boltzmann equation for strongly correlated systems: Comparison to dynamical mean field theory, *Phys. Rev. B* **98**, 134312 (2018).
- [16] J.-P. Joost, N. Schlünzen, and M. Bonitz, G1-G2 scheme: Dramatic acceleration of nonequilibrium Green functions simulations within the Hartree-Fock generalized Kadanoff-Baym ansatz, *Phys. Rev. B* **101**, 245101 (2020).
- [17] M.-B. Tran and Y. Pomeau, Boltzmann-type collision operators for Bogoliubov excitations of Bose-Einstein condensates: A unified framework, *Phys. Rev. E* **101**, 032119 (2020).
- [18] R. Aquino and D. G. Barci, Exceptional points in Fermi liquids with quadrupolar interactions, *Phys. Rev. B* **100**, 115117 (2019).
- [19] B. Kain and H. Y. Ling, Nonequilibrium states of a quenched Bose gas, *Phys. Rev. A* **90**, 063626 (2014).
- [20] T. M. Mishonov, G. V. Pachov, I. N. Genchev, L. A. Atanasova, and D. Ch. Damianov, Kinetics and Boltzmann kinetic equation for fluctuation Cooper pairs, *Phys. Rev. B* **68**, 054525 (2003).
- [21] M. P. Telenkov, Yu. A. Mityagin, V. V. Agafonov, and K. K. Nagaraja, Mechanism of energy relaxation in the system of Landau levels in quantum wells, *JETP Letters* **102**, 678 (2015).
- [22] M. P. Telenkov, Yu. A. Mityagin, T. N. V. Doan, and K. K. Nagaraja, Kinetics of intrasubband electron energy relaxation in quantum wells in a quantizing magnetic field, *Physica E* **104**, 11 (2018).
- [23] P. F. Kartsev, Effective simulation of kinetic equations for bosonic system with two-particle interaction using OpenCL, *Proceedings of IWOCCL'17*, 28 (2017).
- [24] P. F. Kartsev and I. O. Kuznetsov, Simulation of the weakly interacting Bose gas relaxation for cases of various interaction types, *J. Phys.: Conf. Ser.* **936**, 012055 (2017).
- [25] S. W. Smith, *The Scientist and Engineer's Guide to Digital Signal Processing, Second Edition* (California Technical Publishing, 1999), p. 118.
- [26] T. Ando, A. B. Fowler, and F. Stern, Electronic properties of two-dimensional systems, *Rev. Mod. Phys.* **54**, 437 (1982).
- [27] S. T. Beliaev, Energy-spectrum of non-ideal Bose gas, *Zh. Eksp. Teor. Fiz.* **34**, 433 (1958) [*Sov. Phys. JETP* **7**, 299 (1958)].
- [28] S. Giorgini, Damping in dilute Bose gases: A mean-field approach, *Phys. Rev. A* **57**, 2949 (1998).
- [29] L. P. Pitaevskii and S. Stringari, Landau damping in dilute Bose gases, *Phys. Lett. A* **235**, 398 (1997).
- [30] V. V. Kabanov, Electron-electron and electron-phonon relaxation in metals excited by optical pulse, *Low Temp. Phys.* **46**, 414 (2020).
- [31] S. Trotzky, Y.-A. Chen, A. Flesch, I. P. McCulloch, U. Schollwöck, J. Eisert, and I. Bloch, Probing the relaxation towards equilibrium in an isolated strongly correlated one-dimensional Bose gas, *Nature Physics* **8**, 325 (2012).